PCCP

Accepted Manuscript

ROYAL SOCIETY OF CHEMISTRY

www.rsc.org/pccp

Towards a Rationalization of Catalytic Activity Values by means of Local Hyper–Softness on the Catalytic Site. A Criticism About the Use of Net Electric Charges

Jorge Ignacio Martínez-Araya[•♯ 1], **André Grand**[§* 2], **Daniel Glossman-Mitnik**[†3]

[•]*Departamento de Ciencias Químicas, Facultad de Ciencias Exactas, Universidad Andres Bello, Av. República 230, Código Postal 8370134, Tel: +56 2 26618226, Santiago, Chile.*

[♯]*Millennium Nucleus Chemical Processes and Catalysis (CPC), Laboratorio de Química Teórica Computacional (QTC), Facultad de Química, Pontificia Universidad Católica de Chile, Av. Vicuña Mackenna 4860, Casilla 306, Correo 22, Santiago, Chile.*

[§]*Dirección de Postgrado e Investigación, Sede Providencia, Universidad Autónoma de Chile, Carlos Antúnez 1920, Código Postal 7500566, Providencia–Santiago, Chile.*

[*]*Univ. Grenoble Alpes, INAC, SCIB, F-38000, Grenoble, France. CEA, INAC, SCIB, F-38000 Grenoble, France.*

[†]*Laboratorio virtual NANOCOSMOS, Departamento de Medio Ambiente y Energía, Centro de Investigación en Materiales Avanzados, Miguel de Cervantes 120,*

[1]email: Corresponding author jorge.martinez@unab.cl
[2]email: andre.grand@cea.fr
[3]email: daniel.glossman@cimav.edu.mx

Complejo Industrial Chihuahua, Chihuahua, Chih 31136, México.

Abstract

By means of the By means of the Spin–Polarized Conceptual Density Functional Theory (SP–CDFT), three 2,6-bis(imino)pyridine catalysts based on iron(II), used for polymerization of ethylene, were studied. The catalysts differed by substituent group, bearing either -H, -NO_2 or -OCH_3. Up to now, catalytic activity, a purely experimental parameter measuring the mass of polyethylene produced per millimole iron per time and pressure unit at a fixed temperature, has not been explained in terms of local hyper-softness. The latter is a purely theoretical parameter designed for quantifying electronic effects; it is measured using the metal atom responsible for the coordination process with the monomer (ethylene). Because steric effects are not relevant in these kinds of catalysts and only electronic effects drive the catalytic process, an interesting link is found between catalytic activity and the local hyper-softness condensed on the iron atom by means of four functionals (B3LYP, BP86, B97D, and VSXC). This work demonstrates that use of local hyper–softness, predicted by the SP–CDFT, is a suitable parameter for explaining order relationships among catalytic activity values, thus quantifying the electronic influence of the substituent group inducing this difference; use of only net electric charge does not lead to clear conclusions. This finding can aid in estimating catalytic activities leading to a more rational design of new catalysts via computational chemistry.

Keywords: Non–Metallocene Catalysts, BIMP-Fe, Local Reactivity, Spin–Polarized Conceptual Density Functional Theory (SPCDFT), Catalytic Activity

1 Introduction

Group 4 metallocene methyl cations coming from respective pre–catalysts bearing chlorine atoms have been used to catalyze ethylene polymerization reaction which has been well studied from both points of view: theoretical and experimental.[1–12] It is well–known that the polymerization reaction is initiated with a Lewis acid that is known as a co–catalyst which is able to replace chlorine atoms by one methyl group to produce the respective metallocene methyl cation (the active species), being methylaluminoxane the most famous co–catalyst (MAO).[1–3] In 1998, a non–metallocene catalysts was synthesized by Brookhart and Gibson independently. They discovered that MAO–activated iron bis(imino)pyridine yielded activities that were as high as those of group 4 metallocenes aforementioned, also activated by MAO.[13–16] However, some doubts about the oxidation state of iron arose some years ago, so that a first preliminary theoretical work focused on oxidation state in bin(imino)pyridine catalysts. From that study, it was concluded that Fe^{3+} should be a more suitable species rather than Fe^{2+} for catalyzing the polymerization process.[17] A more extended theoretical work[18] supported the results mentioned before, so that it seems that Fe^{3+} makes easier the coordination of ethylene, thus driving the polymerization process through coordination reactions with ethylene molecules.

A neutral dichloro 2,6-bis(imino)pyridine iron compound (Cl_2BIMP-Fe) is the starting material to generate the catalyst, such compound is well-known as a pre-catalyst, meaning a non-catalytic compound that, through an activation process, is trans-

formed into a cationic species which is the catalyst for the polymerization process. In this work the analysis has been focused on the cationic species alone (BIMP-Fe cation, the catalytic species; please see Figures 1 and 2) without taking into account neither the co–catalyst nor the solvent effect because the interest is oriented toward the intrinsic local reactivity of these catalytic species by themselves. For this reason the presence of the co-catalyst has been suppressed in this work, in addition it is known that its computational modelling is still a matter of debate;[19–22] in other words, the co-catalyst is not an issue of interest in this work. The ethylene monomer has also been excluded from this work because its nature is not an explicit focus of attention either. So, if our interest is centered on looking for an approximation to the catalytic activity from the quantum chemistry point of view, then the entire study must be oriented toward the catalyst *per se*.

In 2010, G.H. Zohuri *et al*[23] reported synthesis, characterization and ethylene polymerization behavior of two late transition metal 2,6-bis(imino)pyridine catalysts based on iron(II) of the type $[\mathrm{Y{-}LFe(II)Cl_2}]$ where $-\mathrm{Y} \in \{-\mathrm{NO_2}, -\mathrm{OCH_3}\}$ as depicted by Figures 1 and 2; $\mathrm{Y} = \mathrm{H}$ is used as a control-catalyst. Each can be turned into a BIMP-Fe cation as aforementioned. The substituent $-\mathrm{Y} \in \{-\mathrm{H}, -\mathrm{NO_2}, -\mathrm{OCH_3}\}$ was located at the *para* position of the pyridine ring, and they obtained catalytic activity values as quoted in Table 1; they suggested that the more electron–withdrawing $-\mathrm{Y}$ substituent leads to a higher catalytic activity; according with them and under the assumption that interactions between catalysts and monomer are mainly of electrostatic nature, the lower is the net charge on the metal, the higher is the catalytic

activity of the polymerization.

Table 1: Catalytic activities measured in kilograms of poliethylene per mmol of Fe (where mmol means millimol), per hour and bar at a fixed temperature are reported according to each substituent group $-\mathrm{Y} \in \{-\mathrm{H}, -\mathrm{NO_2}, -\mathrm{OCH_3}\}$ have been obtained by Zohuri *et al.*[23] Polymerization conditions for obtaining these values are the following: ethylene pressure= 5 bar; time= 30 min; solvent=toluene; temperature=30°C; [Fe] = $0.3 \cdot 10^{-3}$mmol.

	-H	**-NO_2**	**-OCH_3**
Cat. Act.	22.750	25.500	18.750

However, since ethylene is a neutral molecule, the interaction with the catalytic species should be of covalent nature rather than electrostatic. This work provided a good chance for testing a local reactivity descriptor that has been designed to measure the most favourable sites for nucleophilic and electrophilic regions due to covalent interactions. Such local reactivity descriptor might be used for prediction or for estimating qualitatively values of catalytic activities of catalysts of the type BIMP-Fe that have not been synthetized yet. These type of catalysts are appropriate for our purposes because the coordination site is not influenced by steric effects coming from the same catalyst at all. In consequence the hypothesis lies in the fact that the use of this local reactivity descriptor (LHS) would lead to a better statistical correlation with the catalytic activity in comparison with the use of the net charge on the iron atom or other type of local reactivity descriptor.

This article is schematized as follows: first, the Theory section will give the reader sufficient information about the aforementioned descriptor of local reactivity that

has been employed in this work; secondly, the Computational Details section indicates the methodologies that have been used to obtain the condensed local hyper–softness values. Third, Results and Discussions section provides the critical analysis concerning to this research. Conclusions are given in the last section.

2 Theory

As a general and intuitive chemical rule, the unfavorable influence of steric effects exerted by a substituent group belonging to a same type of catalyst can be inferred in the sense that a decrease of the catalytic activity is expected as a result of a presence of a bulky substituent group which blocks the coordination site under analysis; this deduction can only be described after watching the molecular model of the structure under analysis. Since a quantification of steric effects is still a matter of debate, although some efforts have been carried out in order to quantify steric effects accurately[24–30] and there is no a unique procedure to carry out an estimation of them, we have priorized the analysis of electronic effects on catalytic activity. The latter is founded in the fact that, after watching the molecular structure under analysis, we realized that there is a predominance of the electronic effect given by the para position of $-$Y substituent instead of its steric effect and in consequence, we can assume that any analysis concerning to the reactivity of such compound should be leaded by the study of possible electronic effects, as presented in this work provided that the $-$Y substituent is the only variable to be taken under consideration; in

other words, catalytic systems that have been chosen at the present work possess its substituent group located pretty far from the coordination site thus implying a constant and negligible steric effect in comparison with electronic effects which are suspected that are mainly responsible on the catalytic behavior of these systems.

2.1 Local Hyper–Softness: A Suitable Local Reactivity Descriptor

Once defined the priority on electronic effects rather than steric ones, we must decide about the type of electronic effect on which the attention should be paid during the theoretical investigation. A BIMP-Fe cation is able to coordinate an olefin (the monomer) due to a mix of both electrostatic and covalent interactions. Electrostatic interactions operate at a long–range distance between π–electrons of the monomer and the BIMP-Fe cation, while covalent interactions operate at a short–range distance, thus involving a displacement of π–electrons towards to the iron atom of the catalyst in order to form a covalent bond that explains the coordination onto the iron atom. Under this perspective, the BIMP-Fe cation undergoes a nucleophilic attack controlled by a covalent interaction rather than electrostatic one. Hence the covalent interaction must be described by means of a suitable local reactivity descriptor.

According to the subsection 2, when covalent interactions are more relevant than electrostatic ones, like this case, and within the framework of Conceptual DFT,[31–36] Morell *et al.*[37–41] have proposed the so–called dual descriptor (DD) which is a local

reactivity descriptor represented as $f^{(2)}(\mathbf{r})$ within the context of closed–shell systems; from the point of view of the electronic density, this is a derivative of second order with respect to number of electrons N and from the point of view of the total energy, this descriptor is a derivative of third order: once as a functional derivative with respect to external potential, $\upsilon(\mathbf{r})$ and twice with respect to the number of electrons, N.[42]

One advantage of $f^{(2)}(\mathbf{r})$ is its capability to reveal, unambiguously, the most nucleophilic and electrophilic sites on a molecule at the same time. A third mathematical interpretation indicates that it corresponds to a derivative of the Fukui function, $f(\mathbf{r})$,[34,43] with respect to the number of electrons, N. The Maxwell relation allows one to understand this local reactivity descriptor as the variation of η (the molecular hardness which measures the resistance to charge transfer[34,44,45]) with respect to the variation of $\upsilon(\mathbf{r})$, the external potential aforementioned. The definition of $f^{(2)}(\mathbf{r})$ is shown as indicated by Morell *et al.*:[37,46]

$$f^{(2)}(\mathbf{r}) = \left(\frac{\partial f(\mathbf{r})}{\partial N}\right)_{\upsilon(\mathbf{r})} = \left[\frac{\delta\eta}{\delta\upsilon(\mathbf{r})}\right]_{N}. \qquad (1)$$

DD reveals, simultaneously, the preferably sites for nucleophilic attacks ($f^{(2)}(\mathbf{r}) > 0$) and the preferably sites for electrophilic attacks ($f^{(2)}(\mathbf{r}) < 0$) into the system at point $\mathbf{r}$. The robustness of DD has been demonstrated through predicting specific sites of nucleophilic and electrophilic attacks in a much more efficient way than the Fukui function by itself[47] because $f^{(2)}(\mathbf{r})$ is able to distinguish those sites of true nucleophilic and electrophilic behavior. As a proof of this characteristic, some works have been published with the aim of highlighting the powerfulness of $f^{(2)}(\mathbf{r})$ and all those local reactivity descriptors that depend on dual descriptor.[38–41,48–50]

An operational formula to obtain DD is given by the arithmetic difference between nucleophilic and electrophilic Fukui functions.[37] When using the most accurate mathematical expression to compute this descriptor as a scalar field (the finite difference approximation method), Eq.(2) is obtained. Since this level of approximation implies three quantum chemical computations, meaning the system under study with $N-1$, $N+1$ and N electrons, a second level of approximation has been used for some years where densities of frontier molecular orbitals provide a working equation easier to use which is given by Eq.(3), so that only the original system (N electrons) provides the needed information without taking into account information coming from the systems bearing $N+1$ and $N-1$ electrons:

$$f^{(2)}(\mathbf{r}) \simeq f^{+}(\mathbf{r}) - f^{-}(\mathbf{r}) = \rho_{\mathrm{N+1}}(\mathbf{r}) - 2\rho_{\mathrm{N}}(\mathbf{r}) + \rho_{\mathrm{N-1}}(\mathbf{r}), \quad (2)$$

$$f^{(2)}(\mathbf{r}) \simeq \rho_{\mathrm{L}}(\mathbf{r}) - \rho_{\mathrm{H}}(\mathbf{r}), \quad (3)$$

where densities of LUMO and HOMO are represented by $\rho_{\mathrm{L}}(\mathbf{r})$ and $\rho_{\mathrm{H}}(\mathbf{r})$, respectively. The influence of molecular symmetry over the local reactivity has been demonstrated by means of the fact that Fukui function must conserve the symmetry,[51] in consequence, DD also must do it. Inasmuch as any degeneracy might arise in frontier molecular orbitals, working equations have been adapted to the molecular symmetry.[52,53] An extended mathematical justification about the influence of degeneracy in local reactivity descriptors has been provided in previous publications.[54,55] Fortunately, this is not the case, meaning that there is no degeneracy detected in all of the frontier molecular orbitals belonging to the cationic systems analyzed in the present work.

Within the context of the Spin–Polarized Conceptual Density-Functional Theory,[57–61] $f^{(2)}(\mathbf{r}) \equiv f_{\mathrm{NNN}}(\mathbf{r})$[56] and the Eq.(4) must be used:

$$f_{\mathrm{NNN}}(\mathbf{r}) \simeq \frac{1}{2}\left\{\rho_{\mathrm{L}}^{\alpha}(\mathbf{r}) + \rho_{\mathrm{L}}^{\beta}(\mathbf{r})\right\} - \frac{1}{2}\left\{\rho_{\mathrm{H}}^{\alpha}(\mathbf{r}) + \rho_{\mathrm{H}}^{\beta}(\mathbf{r})\right\} , \tag{4}$$

The condensation-on-atoms of dual descriptor can be performed through an appropriate integration within the k^{th}–atomic domain Ω_k:

$$\int_{\Omega_k} f_{\mathrm{NNN}}(\mathbf{r})\, d\mathbf{r} = f_{\mathrm{NNN}}\left\{\mathrm{k}\right\} . \tag{5}$$

This procedure will be explained in the subsection 2.2. When $f_{\mathrm{NNN}}\left\{\mathrm{k}\right\} > 0$ the process is driven by a nucleophilic attack on atom k which acts as an electrophilic species.

Conversely, when $f_{\mathrm{NNN}}\{\mathrm{k}\} < 0$ the process is driven by an electrophilic attack over atom k which acts as a nucleophilic species. However values of DD become insignificant as the size of molecule increases.

To overcome this intrinsic behavior of $f_{\mathrm{NNN}}\{\mathrm{k}\}$ another local reactivity descriptor has been defined, so that it permits to measure local reactivities according to the molecular size;[41] thus meaning that it allows one to compare local reactivity among different compounds. Such a descriptor is the local hyper–softness (LHS):[40,62–64]

$$s^{(2)}(\mathbf{r}) = \left(\frac{\partial^2 \rho(\mathbf{r})}{\partial \mu^2}\right)_{v(\mathbf{r})} = \frac{f^{(2)}(\mathbf{r})}{\eta^2} - \frac{f(\mathbf{r})\gamma}{\eta^3}\,, \tag{6}$$

where:

$$\gamma = \left(\frac{\partial \eta}{\partial N}\right)_{v(\mathbf{r})} \tag{7}$$

γ is called hyper–hardness whose physical meaning and relevance is under study.[65] Within the context of the Spin–Polarized Conceptual Density-Functional Theory, $s^{(2)}(\mathbf{r}) \equiv s_{\mathrm{NNN}}(\mathbf{r})$.[56]

LHS has been mathematically defined as the additive inverse of the variation of global softness with respect to a change experienced by the external potential at a fixed electronic chemical potential, so that through a Maxwell relation it is also defined as the partial derivative of local softness[62,66–68] with respect to the chemical

potential at a fixed external potential:

$$s^{(2)}(\mathbf{r}) = -\left[\frac{\delta \mathrm{S}}{\delta \upsilon\left(\mathbf{r}\right)}\right]_{\mu} = \left(\frac{\partial s\left(\mathbf{r}\right)}{\partial \mu}\right)_{\upsilon(\mathbf{r})} . \tag{8}$$

In principle, the use of local softness $s(\mathbf{r})$, a local reactivity descriptor corresponding to a derivative of first order of the electronic density with respect to the chemical potential, μ gives rise to both nucleophilic, $s^{+}\left(\mathbf{r}\right)$ and electrophilic, $s^{-}\left(\mathbf{r}\right)$ versions of local softness, so revealing nucleophilic and electrophilic sites, respectively. But as $s^{(2)}(\mathbf{r})$ is also a local reactivity descriptor that corresponds to a derivative of second order of the electronic density with respect to the chemical potential, it will be able to reveal true nucleophilic and electrophilic sites at the same time thus allowing to establish comparisons among local reactivities of molecules of different sizes. The latter is an ability that the dual descriptor does not have since it only gives information about the local reactivity at an intramolecular level because LHS is naturally scaled by global softness squared:

$$\begin{aligned} s^{(2)}(\mathbf{r}) &= \frac{f^{(2)}(\mathbf{r})}{\eta^2} - \frac{f(\mathbf{r})\gamma}{\eta^3}\,, \\ &= f^{(2)}(\mathbf{r})\mathrm{S}^2 - f(\mathbf{r})\mathrm{S}^3\gamma\,, \\ &= \mathrm{S}^2\left\{f^{(2)}(\mathbf{r}) - f(\mathbf{r})\mathrm{S}\gamma\right\}\,. \end{aligned} \tag{9}$$

where S stands for the global softness[33,34,45] which can be calculated in terms of HOMO and LUMO energies provided that the Koopmans' theorem[69] is satisfied as

several articles have demonstrated:[33,34,45]

$$\mathrm{S} \simeq (\varepsilon_{\mathrm{L}} - \varepsilon_{\mathrm{H}})^{-1} \ , \tag{10}$$

where ε_{L} and ε_{H} stand for the the LUMO and HOMO energies, respectively. Nevertheless some doubts about the use of this theorem have been exposed by Joubert[70] because the LUMO computed by means of a conventional Kohn-Sham DFT calculation corresponds to an electronic excitation and not to a capture of electron.[71,72] Even so, the information coming from Koopmans' theorem would provide a valid qualitative picture about molecular reactivity. Nevertheless, some authors have claimed that γ has a chemical meaning,[65] so that a working equation that includes this term should be proposed in the short–term. Notice that LHS is also understood as a third order derivative of the grand potential $\Omega = E - \mu N$: once as a first functional derivative with respect to the external potential, $v(\mathbf{r})$ and twice with respect to the chemical potential, μ.

For a proper use of the SP-CDFT, it is worthwhile to mention that when $s^{(2)}(\mathbf{r})$ is equal to 1 a.u.$\equiv 1\,\mathrm{hartree}^{-2} \cdot \mathrm{bohr}^{-3}$ implies that the local softness, $s(\mathbf{r})$, varies in $1\,\mathrm{hartree}^{-1} \cdot \mathrm{bohr}^{-3}$ because of a change experienced by the chemical potential, μ, in $1\,\mathrm{hartree}$. More details about this deduction of units can be found in the respective citation.[73]

It has been demonstrated that γ is a negligible amount[38,43] in Eq.(6), meaning that

$f^{(2)}(\mathbf{r}) >> f(\mathbf{r})\mathrm{S}\gamma$ and the Eq.(9) can be written as follows:

$$s^{(2)}(\mathbf{r}) \simeq f^{(2)}(\mathbf{r})\mathrm{S}^2\,, \tag{11}$$

At the moment, the use of Eq.(11) is sufficient for the purpose of this work where $s^{(2)}(\mathbf{r})$ is computed by the use of Eqs.(3) and (10). However for open–shell systems, the Eq.(4) must be used under the frontier molecular orbital approximation along with the following expression:

$$\mathrm{S_{NN}} \simeq \left\{ \frac{\varepsilon_{\mathrm{L}}^{\alpha} + \varepsilon_{\mathrm{L}}^{\beta}}{2} - \frac{\varepsilon_{\mathrm{H}}^{\alpha} + \varepsilon_{\mathrm{H}}^{\beta}}{2} \right\}^{-1}\,, \tag{12}$$

where $\mathrm{S_{NN}} = \eta_{\mathrm{NN}}^{-1}$; it is simply the notation that one has to use for open–shell systems instead of S; and η_{NN} is the notation to be used in open–shell systems instead of using the η symbol.

According to all claimed above, the Eq. (11) must be expressed as follows for open–shell systems:

$$s_{\mathrm{NNN}}(\mathbf{r}) \simeq f_{\mathrm{NNN}}(\mathbf{r})\mathrm{S}_{\mathrm{NN}}^2\,, \tag{13}$$

Similarly to dual descriptor, LHS can also be condensed through an appropriate integration within the k^{th}–atomic domain Ω_k:

$$\int_{\Omega_k} s_{\mathrm{NNN}}(\mathbf{r})\, d\mathbf{r} = \mathrm{s_{NNN}}\left\{\mathrm{k}\right\}\,. \tag{14}$$

Then, the use of LHS allows one to make sure the measurement of local reactivity on a molecular system can be comparable with local reactivity of other systems in spite of differences in size. This descriptor should be able to measure electronic effects in agreement with the molecular size.[73] The obtention of integrated values of $s_{\mathrm{NNN}}(\mathbf{r})$ on iron is explained in the Computational Methods section. When the catalytic activity is mainly controlled by electronic effects and not by steric effects, the hypothesis is that a higher condensed value of $\mathrm{s_{NNN}}\,\{\mathrm{Fe}\}$, leads to a higher value of catalytic activity.

2.2 Computational Details

Catalytic systems bearing substituent groups $-\mathrm{Y} = \{-\mathrm{H}, -\mathrm{NO_2}, -\mathrm{OCH_3}\}$ were taken into account at a high–spin configuration (sextet) along with a total net charge of 2+, thus meaning Fe(III) as depicted by Figure 2. Geometrical optimizations were performed for the same cationic complex at a the high–spin configuration (sextet) aforementioned with the LANL2DZ[74–76] with effective core potentials for all atoms by means of the following functionals: The Becke–3 for exchange and Lee–Yang–Parr for correlation B3LYP (a hybrid generalized gradient approximation functional meaning dependence of electronic density and its gradient are included along with an accurate expression for the exchange functional; this is also so–called hybrid GGA functional),[77–80] BP86 (a pure GGA functional),[77,81] B97D (a hybrid GGA functional including an empirical correction dispersion also so–called hybrid GGA+D)[82] and VSXC (a pure meta GGA functional where explicit dependence on kinetic en-

ergy density is included).[83] Frequency calculations were then performed to identify the stationary points as minima.[84] All calculations were carried out using the GAUSSIAN 09[85] software package.

For obtaining integrated values of Fukui function, the Fukui REV 1.1 software was used[86–89] where nucleophilic and electrophilic Fukui functions are condensed as follows:

$$f_k^+ = \sum_{\nu \in k} \sum_{\mu=1}^{M} c_{\nu\,\mathrm{LUMO}}^{*} c_{\mu\,\mathrm{LUMO}} \mathrm{S}_{\nu\mu} \tag{15}$$

$$f_k^- = \sum_{\nu \in k} \sum_{\mu=1}^{M} c_{\nu\,\mathrm{HOMO}}^{*} c_{\mu\,\mathrm{HOMO}} \mathrm{S}_{\nu\mu}\,. \tag{16}$$

where $\mathrm{S}_{\nu\mu} = \int \mathrm{d}\mathbf{r} \chi_\nu^*(\mathbf{r}) \chi_\mu(\mathbf{r})$ is the overlap integral where $\chi_\mu(\mathbf{r})$ is an atomic basis function and $\chi_\nu^*(\mathbf{r})$ is a conjugate atomic basis function in which $\nu \in k$ indicates that the sum runs over all of atomic basis functions that are centered on atom k under the assumption that there are M atomic basis functions. As indicated by Eqs.(15) and (16), this software works under the frontier molecular orbital approximation so

that the condensation scheme is explained as follows:

$$\begin{aligned} f^{+}(\mathbf{r}) &= \rho(\mathbf{r})_{N+1} - \rho(\mathbf{r})_{N} \\ &\approx |\psi\,(\mathbf{r})|^{2}_{\mathrm{LUMO}} = \sum_{\nu=1}^{M}\sum_{\mu=1}^{M} c^{*}_{\nu\ \mathrm{LUMO}} c_{\mu\ \mathrm{LUMO}} \chi^{*}_{\nu}(\mathbf{r})\chi_{\mu}(\mathbf{r}) \end{aligned} \tag{17}$$

$$\begin{aligned} f^{-}(\mathbf{r}) &= \rho(\mathbf{r})_{N} - \rho(\mathbf{r})_{N-1} \\ &\approx |\psi\,(\mathbf{r})|^{2}_{\mathrm{HOMO}} = \sum_{\nu=1}^{M}\sum_{\mu=1}^{M} c^{*}_{\nu\ \mathrm{HOMO}} c_{\mu\ \mathrm{HOMO}} \chi^{*}_{\nu}(\mathbf{r})\chi_{\mu}(\mathbf{r})\,. \end{aligned} \tag{18}$$

Since dual descriptor is the arithmetic difference between $f^{+}(\mathbf{r})$ and $f^{-}(\mathbf{r})$, the condensed value of $f^{(2)}(\mathbf{r})$ is the arithmetic difference between Eq.(16) and Eq.(15):

$$f_{k}^{(2)} = \sum_{\nu\in k}\left\{\sum_{\mu=1}^{M} c^{*}_{\nu\ \mathrm{LUMO}} c_{\mu\ \mathrm{LUMO}} \mathrm{S}_{\nu\mu} - \sum_{\mu=1}^{M} c^{*}_{\nu\ \mathrm{HOMO}} c_{\mu\ \mathrm{HOMO}} \mathrm{S}_{\nu\mu}\right\}. \tag{19}$$

Finally, the condensed value of local hyper–softness is simply obtained by the following multiplication: $\mathrm{S}^{2}\, f_{k}^{(2)}$, or $\mathrm{S}^{2}_{\mathrm{NN}}\, f_{\mathrm{NNN}}\,\{k\}$ within the context of open–shell systems, meaning that all of the condensed values of dual descriptor are computed as a simple arithmetic difference between $f^{+}_{\mathrm{NN}}\{\mathrm{Fe}\}$ and $f^{-}_{\mathrm{NN}}\{\mathrm{Fe}\}$, respectively in order to obtain $f_{\mathrm{NNN}}\{\mathrm{Fe}\}$. Condensed values of $\mathrm{s}_{\mathrm{NNN}}\{\mathrm{Fe}\}$ are obtained as an ordinary multiplication between S^{2} and $f_{\mathrm{NNN}}\{\mathrm{Fe}\}$. Note that the notation $f^{+}_{\mathrm{NN}}\{\mathrm{Fe}\}$, $f^{-}_{\mathrm{NN}}\{\mathrm{Fe}\}$, $f_{\mathrm{NNN}}\{\mathrm{Fe}\}$ and $\mathrm{s}_{\mathrm{NNN}}\{\mathrm{Fe}\}$ is applied within the context of open–shell systems only.

Concerning to electric net charges on iron atom, they were computed for each cationic complex, by means of the Mülliken, Natural[90] and CHELPG[91] population

analysis, respectively, to test that local hyper–softness is a better parameter to link with catalytic activity rather than the net charge on iron atom. When CHELPG was used, the following atomic radii were considered: Fe, 0.64 Å; H, 1.31 Å; N, 1.71 Å; O, 1.40 Å; C, 1.38 Å. The use of net charges coming from the CHELPG scheme as a type of local reactivity descriptor were considered in this work for the same reason that net charges by means of Mülliken and NPA were taken into account too: to test its capability to establish a link with catalytic activity, however there is an additional precedent that support the CHELPG scheme to be selected. That precedent indicates that condensed Fukui functions within the CHELPG scheme through a finite difference approximation (Yang and Mortier)[92] gives so good results as those given by the AIM scheme (and better than Mülliken),[93] so it sounds sensible to perform a test by simply using the net charges obtained by CHELPG. Then the reader has to notice that we are then comparing three types of charges, which should be more simple to obtain than condensed Fukui functions based on Mülliken's scheme which are computed through the Fukui software available for free.

Some question arise, for instance, are any of these three schemes to give net charges on atoms as local reactivity descriptors good enough to rationalize values of catalytic activity or should we resort for a more sophisticated tool like Fukui functions, dual descriptor and local hyper–softness condensed each on atoms? and if so, which of them should be used as a suitable local reactivity descriptor: Fukui functions, local softness or local hyper–softness? This article aims to unravel this uncertainty because there is a plethora of reactivity descriptors that might confuse to novel

users about their capabilities. The first intuitive idea is to use net charges on atoms under the assumption that electrostatic interactions are ruling the chemical process under analysis, but if net charges do not show a link with the chemical process under study, what kind of another local reactivity descriptor should be used? the local hyper–softness might reply that question provided that covalent interactions are the responsible of driving the reaction under study, in this case the reaction under study is the coordination between an olefin like ethylene and the metallic atom of an organometallic catalytic cation complex based on iron which give rise to the catalytic cycle to produce polyethylene.

3 Results and Discussion

As the electronic effect predominates over the steric effect as expected in this group of catalysts, a link is expected between the condensed value of the LHS on the iron atom and the catalytic activity of the respective catalyst. This would provide a rational explanation about the found differences among catalysts mainly in terms of electronic effects. But first, let us check the performance of the net charge on the iron atom as a plausible local reactivity descriptor to rationalize the catalytic activity.

Zohuri *et al.*[23] provide catalytic activities for these systems as quoted by Table 1 so providing the following order relationship:$-NO_2 > -H > -OCH_3$.

Table 2: Catalytic activity (CatAct) is expressed in kilograms of polyethylene per mmol of Fe, per hour and bar at a fixed temperature where experimental conditions established by obtained by Zohuri *et al.*[23] for polymerization are the following: ethylene pressure= 5 bar; time= 30 min; solvent=toluene; temperature=30°C; [Fe] = $0.3 \cdot 10^{-3}$mmol; electric net charge on iron atom calculated by the Mülliken population analysis (Q_M {Fe}), natural population analysis (Q_{NPA} {Fe}) and the population analysis based on charges that are derived by fitting to a potential electrostatic potential CHELPG (Q_{CHE} {Fe}) are expressed in atomic units.

	CatAct	$\mathbf{Q_M}$ **{Fe}**	$\mathbf{Q_{NPA}}$ **{Fe}**	$\mathbf{Q_{CHE}}$ **{Fe}**
B3LYP:				
-NO_2	25.50	0.489	1.223	2.233
-H	22.75	0.626	1.234	2.272
-OCH_3	18.75	0.643	1.243	2.239
BP86:				
-NO_2	25.50	0.519	1.002	2.213
-H	22.75	0.534	1.015	2.272
-OCH_3	18.75	0.541	1.027	2.245
B97D:				
-NO_2	25.50	0.572	1.090	2.126
-H	22.75	0.582	1.096	2.142
-OCH_3	18.75	0.585	1.103	2.172
VSXC:				
-NO_2	25.50	0.403	1.102	2.170
-H	22.75	0.405	1.106	2.242
-OCH_3	18.75	0.406	1.114	2.297

According to Table 2, Mulliken and NPA population analysis provide net charges on iron atom that follow the reverse order: $-NO_2 < -H < -OCH_3$ no matter the functional being used. The latter suggests a reverse order relationship between catalytic activity and net charge on iron, however, when using the CHELPG population analysis, an anomalous order relationship is obtained with the B3LYP and BP86 functionals: $-NO_2 < -OCH_3 < -H$, meanwhile the B97D and VSXC functionals provide an identical order relationship to that one obtained by the catalytic activity: $-NO_2 > -H > -OCH_3$. Clearly, net charges are not reliable local reactivity descriptors to rationalize an experimental parameter because they fail when using at least three different population analysis combined with four types of functionals of different nature: a hybrid GGA functional, a pure GGA functional, a hybrid GGA+D and a meta GGA functional.

3.1 A Link between Catalytic Activity and Local Hyper–Softness

When $s_{NNN}\{Fe\} > 0$ implies that nucleophilic attacks will be oriented on iron atom; on the contrary, when $s_{NNN}\{Fe\} < 0$ implies that electrophilic attacks will be headed on iron atom. Since the interaction between an ethylene molecule and an iron complex involves a nucleophilic attack of π–electrons coming from ethylene toward to the iron atom in the complex cation to give rise the Cossée–Arlman's complex, this π–complex experiences a noticeable intramolecular rearrangement in such a way that the methyl group, originally linked to iron migrates toward to one of the carbon

atoms of the coordinated ethylene thus leading to a propyl chain, thus setting free the coordination site again on iron atom which will allow a coordination of a second ethylene molecule and so on. This is the essential process that explains the increase of the carbon chain length along the entire polymerization process when a catalyst is present. Tables 3 and 4 give the needed numbers to compute condensed values of LHS on the iron atom:

Table 3: Values of energies of α-HOMO ($\varepsilon_{\mathrm{H}}^{\alpha}$), β-HOMO ($\varepsilon_{\mathrm{H}}^{\beta}$), α-LUMO ($\varepsilon_{\mathrm{L}}^{\alpha}$), β-LUMO ($\varepsilon_{\mathrm{L}}^{\beta}$) and molecular hardness (η_{NN}), all of them are expressed in eV.

	$\varepsilon_{\mathrm{H}}^{\alpha}$	$\varepsilon_{\mathrm{H}}^{\beta}$	$\varepsilon_{\mathrm{L}}^{\alpha}$	$\varepsilon_{\mathrm{L}}^{\beta}$	η_{NN}
B3LYP:					
-NO_2	-0.44411	-0.44575	-0.35931	-0.38788	1.9411
-H	-0.43617	-0.4381	-0.33624	-0.37567	2.2090
-OCH_3	-0.43011	-0.43274	-0.32397	-0.36716	2.3364
BP86:					
-NO_2	-0.41237	-0.42600	-0.36919	-0.41052	0.7981
-H	-0.40272	-0.41761	-0.35043	-0.40053	0.9438
-OCH_3	-0.39493	-0.41185	-0.34019	-0.39356	0.9936
B97D:					
-NO_2	-0.41219	-0.42135	-0.36639	-0.40306	0.8720
-H	-0.40229	-0.41281	-0.34705	-0.39359	1.0131
-OCH_3	-0.39431	-0.40688	-0.33599	-0.38723	1.0608
VSXC:					
-NO_2	-0.42188	-0.42821	-0.36966	-0.40967	0.9627
-H	-0.41234	-0.41976	-0.3494	-0.39955	1.1313
-OCH_3	-0.4059	-0.41477	-0.33846	-0.39350	1.2070

Rigorously speaking, molecular hardness is expressed in atomic unit of energy per atomic unit of charge squared, thus implying a.u. of energy $\cdot$ (a.u. of charge)$^{-2}$ = hartree $\cdot$ (a.u. of charge)$^{-2}$ $\equiv$ hartree. and for that reason molecular hardness is usually expressed only in units of energy, however the unit of charge is included too,

but in atomic units.

Table 4: Condensed values on iron of: nucleophilic Fukui function ($f^{+}_{NN}\{Fe\}$), electrophilic Fukui function ($f^{-}_{NN}\{Fe\}$), dual descriptor ($f_{NNN}\{Fe\}$), nucleophilic local softness ($s^{+}_{NN}\{Fe\}$), electrophilic local softness ($s^{-}_{NN}\{Fe\}$), local hyper–softness (LHS, $s_{NNN}\{Fe\}$), global softness (S_{NN}) and global softness squared (S^{2}_{NN}). The condensed Fukui functions (nucleophilic and electrophilic) are dimensionless, no matter the unit we are using for the respective Fukui functions, condensed dual descriptor is expressed in (a.u. of charge)$^{-1}$ which is understood as a dimensionless unit in practice, condensed local softnesses are expressed in eV^{-1}, condensed LHS is expressed in m(eV^{-2}), global softness is expressed in eV^{-1} and global softness squared is expressed in eV^{-2}.

	$f^{+}_{NN}\{Fe\}$	$f^{-}_{NN}\{Fe\}$	$f_{NNN}\{Fe\}$	$s^{+}_{NN}\{Fe\}$	$s^{-}_{NN}\{Fe\}$	$s_{NNN}\{Fe\}$	S_{NN}	S^{2}_{NN}
B3LYP:								
-NO_2	0.2654	0.0244	0.2410	0.1367	0.0126	63.96	0.5152	0.2654
-H	0.3099	0.0279	0.2820	0.1403	0.0126	57.79	0.4527	0.2049
-OCH_3	0.3328	0.0626	0.2702	0.1424	0.0268	49.50	0.4280	0.1832
BP86:								
-NO_2	0.3317	0.1341	0.1976	0.4156	0.1680	310.22	1.2530	1.5699
-H	0.3490	0.1382	0.2108	0.3698	0.1464	236.65	1.0595	1.1226
-OCH_3	0.3481	0.1377	0.2104	0.3503	0.1386	213.12	1.0064	1.0129
B97D:								
-NO_2	0.3800	0.1290	0.2510	0.4358	0.1479	330.10	1.1468	1.3151
-H	0.3868	0.1309	0.2560	0.3818	0.1292	249.42	0.9871	0.9743
-OCH_3	0.3870	0.1268	0.2603	0.3648	0.1195	231.32	0.9427	0.8887
VSXC:								
-NO_2	0.3446	0.1188	0.2258	0.3580	0.1234	243.64	1.0387	1.0790
-H	0.3565	0.1239	0.2326	0.3151	0.1095	181.74	0.8839	0.7813
-OCH_3	0.3639	0.1339	0.2300	0.3015	0.1109	157.87	0.8285	0.6864

Observe that $f^{+}_{\mathrm{NN}}\{\mathrm{Fe}\} > f^{-}_{\mathrm{NN}}\{\mathrm{Fe}\}$ and $\mathrm{s}^{+}_{\mathrm{NN}}\{\mathrm{Fe}\} > \mathrm{s}^{-}_{\mathrm{NN}}\{\mathrm{Fe}\}$ is always satisfied, thus indicating that the iron atom is ready to receive a nucleophilic attack preferably rather than an electrophilic attack. The use of $f^{-}_{\mathrm{NN}}\{\mathrm{Fe}\}$ and $\mathrm{s}^{-}_{\mathrm{NN}}\{\mathrm{Fe}\}$ makes no sense.

To obtain values of global softness, first the molecular hardness must be computed, in agreement with Eq.(12), values of frontier molecular orbitals α and β are needed which lead to molecular hardness value as Table 3 shows.

According to these results, in particular the $\mathrm{s}_{\mathrm{NNN}}\{\mathrm{Fe}\}$ column of Table 4, it is revealed that there is a link between catalytic activity and local hyper–softness condensed on the iron atom when iron has a 3+ oxidation state and a sextet spin–multiplicity. The reader can notice that the order relationship is conserved for these four functionals: $-\mathrm{NO}_2 > -\mathrm{H} > -\mathrm{OCH}_3$.

However, notice that LHS as well as electric net charges on iron atoms are methodologically and functional–dependant, meaning these values are influenced by level of theory, even if the order relationship is conserved as the $\mathrm{s}_{\mathrm{NNN}}\{\mathrm{Fe}\}$ case. The magnitudes of LHS are pretty similar between the BP86 and B97D functionals, but they differ in comparison with values given by the VSXC functional and they are extremely different when comparing with the results coming from the B3LYP functional. Nevertheless there is a way to figure out if LHS is a better local reactivity descriptor to support experimental values as catalytic activities, because the

conservation of the order relationship of LHS is a positive signal to think that this descriptor is more convenient rather than using net charges (and other descriptors).

In principle, if so, then a proportionality between LHS condensed on iron atom and catalytic activity should be suggested rather than between net charge and catalytic activity, however there is still an important detail that prevents to directly establish this comparison yet: The order of magnitude. For each functional used in this work, catalytic activity, local hyper–softness condensed on iron atom and net charge on iron atom exhibit differences in their orders of magnitude. Among different functionals, local hyper–softness presents differences in their orders of magnitude, for instance, there is a difference of one order of magnitude between local hyper–softness computed by means of the B3LYP functional and the one calculated by the BP86 functional as exhibited by Table 2.

To assess a possible connection between the local hyper–softness with the catalytic activity and the net charge and the catalytic activity, all values of these parameters were converted into a type of value of one order of magnitude as indicated by Table 5. Each set of three values of condensed LHS on the iron atom, for the same functional, was divided by the smallest value in order to turn them to relative values. And to establish a fair comparison, the same transformation procedure was performed on net charges, Fukui functions, dual descriptor, local softness, global softness and global softness squared. To better understand this method, let us see an example: From Table 2 we took the catalytic activities (25.50, 22.75 and 18.75)

to be divided by 18.75 so leading to relative values of catalytic activities quoted in Table 5; in addition, the condensed LHS coming from the use of the B3LYP functional are taken from Table 4 (47.36, 42.79 and 36.65) and they are divided by 36.65 so leading to the relative condensed LHS values reported in Table 5 (1.292, 1.168 and 1.000). After repeating this procedure for the remaining functionals, the Table 5 is completed with: relative local hyper–softness values and relative net charges values thus allowing to generate bar graphics as depicted by Figures 3 and 4. Please check the Supporting Information where relative values for all of the descriptors quoted in Tables 3 and 4 are graphically represented and, as observed, local hyper–softness is the best descriptor to explain an experimental parameter like catalytic activity.

Observe that, according to Figure 3, a possible proportionality between catalytic activity and electric net charge on iron atom is discarded; on the contrary, there is a proportionality that might be established between catalytic activity and local hyper–softness condensed on the iron atom as depicted by Figure 4. This makes sense since the interaction that rules the flux of π–electrons coming from the olefin toward the iron atom is of covalent nature mainly rather than electrostatic nature and LHS is a proper local reactivity descriptor that permits a quantification of reactivity of sites that are susceptible to be covalently attacked by nucleophilic and electrophilic reagents. In Supporting Information it is possible to observe, qualitatively through the bar graphics, that LHS is a better local reactivity descriptor than net charges, nucleophilic Fukui function, dual descriptor, nucleophilic local softness, global softness and global softness squared.

Table 5: Relative values of catalytic activity, local hyper–softness and electric net charges defined in the previous table are dimensionless and they are symbolically represented by r-CatAct, r-s_{NNN} {Fe}, r-Q_{M} {Fe}, r-Q_{NPA} {Fe} and r-Q_{CHE} {Fe}.

	r-CatAct	**r-s_{NNN} {Fe}**	**r-Q_{M} {Fe}**	**r-Q_{NPA} {Fe}**	**r-Q_{CHE} {Fe}**
B3LYP:					
-NO_2	1.360	1.292	1.000	1.000	1.000
-H	1.213	1.168	1.280	1.008	1.018
-OCH_3	1.000	1.000	1.315	1.016	1.003
BP86:					
-NO_2	1.360	1.456	1.000	1.000	1.000
-H	1.213	1.110	1.029	1.013	1.027
-OCH_3	1.000	1.000	1.043	1.025	1.015
B97D:					
-NO_2	1.360	1.427	1.000	1.000	1.000
-H	1.213	1.078	1.018	1.006	1.007
-OCH_3	1.000	1.000	1.023	1.012	1.022
VSXC:					
-NO_2	1.360	1.543	1.000	1.000	1.000
-H	1.213	1.151	1.006	1.004	1.033
-OCH_3	1.000	1.000	1.008	1.010	1.058

4 Conclusions

In the field of catalysis driven by BIMP-Fe cations for polymerization process of ethylene, and in reference to the electronic effects, the main advantage of using the local hyper–softness descriptor, $s_{NNN}\{Fe\}$ for open–shell systems which is condensed on a strategic site of the catalytic system, lies in the fact that this is a function that is consistent–size, thus allowing to establish comparisons of local reactivity among catalytic systems of different sizes; this is not possible to carry out with the dual descriptor by itself.

On the other hand, although the measure of steric effects is still an issue of debate, fortunately, the set of catalytic systems that have been theoretically studied at the present work lacks to exhibit a dramatic influence of this type of effect by the $-Y$ substituent group, so that the main effect of the substituent group is attributable to electronic aspects given by the electron-withdrawing or electron-donor behavior solely. In consequence an experimental key parameter as the catalytic activity has been explained in terms of the local hyper–softness (LHS), a theoretical parameter, which has turned out to be better than the use of net charge on iron atom thus supporting the predominantly covalent nature of the interaction catalyst–monomer rather than electrostatic.

Furthermore, condensed LHS on iron atom has demonstrated to be a more robust conceptual tool than global softness, global softness squared, electric net charge, nucleophilic Fukui function, nucleophilic local softness and dual descriptor on iron atom since the found trend between catalytic activity and LHS condensed on iron atom is well conserved in spite of using four functionals.

The influence of variables like temperature, solvent, pressure of monomer and concentration of catalyst have been considered as constant parameters, however authors of the present work are aware on the fact that these parameters could also be analyzed in terms of some other proper reactivity descriptors. At the moment, to make sure that the influence of substituent groups on catalytic activity can be predictable through the use of the local hyper–softness, more values of catalytic activities are required along with constant remaining experimental conditions under the assumption that steric effects are irrelevant and the interaction that rules the entire catalytic process is mainly of covalent nature. In absence of steric effects, or when it is suspected that they are not playing an essential role during a chemical interaction, the use of LHS should be suitable to measure electronic effects which can be responsible of values of catalytic activity due to the degree of covalent character that is ruling the interaction under analysis and not the use of net charges because it does not give a proper answer that helps understand catalytic activity values.

To sum up, an important consequence of the research reported here is having the chance to not only explain differences among catalytic activities measured under the same experimental conditions, but also estimate values of catalytic activities of new BIMP-Fe cations when −Y, the substituent group, is changed by another one that has never been put on such position before, provided that the experimental conditions are the same than that were defined for those known BIMP-Fe cations. LHS is a key parameter that can contribute to a rational computational design of new catalysts.

Acknowledgments

J.I. Martínez-Araya wishes to thank to Dr. Pablo Jaque for having fruitful discussions that allowed to improve remarkably the aim of this work. Also authors wish to thank financial support coming from FONDECYT grants N° 11100070 (Project for Initiation into Research), N° 1140289 and *ICM*, Millennium Nucleus Chemical Processes and Catalysis (CPC) grant N° 120082. D. Glossman-Mitnik is a researcher of CIMAV and CONACYT (Mexico) and acknowledges both institutions for partial support. Also the authors thank to Dr. E. Chamorro (UNAB) for providing the computational code Fukui to compute condensed values of nucleophilic and electrophilic Fukui functions (Fukui.Exe, a Visual Basic tool for evaluating global and local reactivity DFT descriptors).

Bibliography

[1] Kaminsky, W.; Külper, K.; Brintzinger, H.H.; Wild, F.R.W.P. Polymerization of Propene and Butene with a Chiral Zirconocene and Methylalumoxane as Cocatalyst. *Angew. Chem. Int. Ed. Engl.* **1985**, *24*, 507–508.

[2] Schuntenhaus, H.; Brintzinger, H.H. 1,1'-Trimethylenebis(η^5 5-3-tert-butylcyclopentadienyl)-titanium(IV)dichloride, a Chiral Ansa-titanocene Derivative. *Angew. Chem. Int. Ed. Engl.* **1979**, *18*, 777–778.

[3] Wild, F.R.W.P.; Zsolnai, L.; Huttner, G.; Brintzinger, H.H. Ansa-metallocene Derivatives : IV. Synthesis and Molecular Structures of Chiral Ansa-titanocene Derivatives with Bridged Tetrahydroindenyl Ligands. *J. Organomet. Chem.* **1982**, *232*, 233–247.

[4] Heiland, K.; Kaminsky, W. Comparison of Zirconocene and Hafnocene Catalysts for the Polymerization of Ethylene and 1-Butene. *Makromol. Chem.* **1992**, *193*, 601–610.

[5] D'Agnillo, L.; Soares, J.B.P.; Penlidis, A. Effect of Operating Conditions on the Molecular Weight Distribution of Polyethylene Synthesized by Soluble Metallocene/Methylaluminoxane Catalysts. *Macromol. Chem. Phys.* **1998**, *199*, 955–962.

[6] Kaminsky, W. New Polymers by Metallocene Catalysis. *Macromol. Chem. Phys.* **1996**, *197*, 3907–3945.

[7] Frauenrath, H. *Polymerization of Olefins and Functionalized Monomers with Zirconocene Catalysts*. Ph.D. Thesis, Fakultät für Mathematik, Informatik und Naturwissenschaften der Rheinisch–Westfälischen Technischen Hochschule Aachen, Deutschland, October **2001**.

[8] Cruz, V.L.; Muñoz-Escalona, A.; Martínez-Salazar, J. A Theoretical Study of the Comonomer Effect in the Ethylene Polymerization with Zirconocene Catalytic Systems. *J. Polym. Sci. Part A: Polym. Chem.* **1998**, *36*, 1157–1167.

[9] Petitjean, L.; Pattou, D.; Ruiz-López, M.F. Theoretical Study of Selectivity Mechanisms in Propylene Polymerization with Metallocene Catalysts. *J. Mol. Struct.–THEOCHEM)* **2001**, *541* , 227–235.

[10] Corradini, P.; Cavallo, L.; Guerra, G. Molecular Modeling Studies on Stereospecificity and Regiospecificity of Propene Polymerization by Metallocenes. In *Metallocene-Based Polyolefins*; Scheirs, J., Kaminsky, W., Eds.; Wiley Series in Polymer Science; John Wiley & Sons Ltd.: Chichester, England, 2000; Vol. 2, pp 3–36.

[11] Woo, T.K.; Deng, L.; Margl, P.M.; Ziegler, T. Computational Modeling of Single-Site Olefin Polymerization Catalysts. In *Metallocene-Based Polyolefins*; Scheirs, J., Kaminsky, W., Eds.; Wiley Series in Polymer Science; John Wiley & Sons Ltd.: Chichester, England, 2000; Vol. 2, pp 69–88.

[12] Martínez Araya, J.I. *Estudio Teórico de la Polimerización de Etileno Catalizada por Catión Metil–Bis(ciclopentadienil)Metaloceno del Grupo IVB*. Ph.D.

Thesis, Facultad de Química, Pontificia Universidad Católica de Chile, Chile, June **2008**.

[13] Small, B.L.; Brookhart, M.; Bennett, A.M.A. Highly Active Iron and Cobalt Catalysts for the Polymerization of Ethylene. *J. Am. Chem. Soc.* **1998**, *120*, 4049–4050.

[14] Small, B.L.; Brookhart, M. Iron-Based Catalysts with Exceptionally High Activities and Selectivities for Oligomerization of Ethylene to Linear α-olefins. *J. Am. Chem. Soc.* **1998**, *120*, 7143–7144.

[15] Britovsek, G.J.P.; Bruce, M.; Gibson, V.C.; Kimberley, B.S.; Maddox, P.J.; Mastroianni, S.; McTavish, S.J.; Redshaw, C.; Solan, G.A.; Strömberg, S.; White, A.J.P.; Williams, D.J. Iron and Cobalt Ethylene Polymerization Catalysts Bearing 2,6-Bis(imino)pyridyl Ligands: Synthesis, Structures, and Polymerization Studies. *J. Am. Chem. Soc.* **1999**, *121*, 8728–8740.

[16] Britovsek, G.J.P.; Gibson, V.C.; McTavish, S.J.; Solan, G.A.; White, A.J.P.; Williams, D.J.; Britovsek, G.J.P.; Kimberley, B.S.; Maddox, P.J. Novel Olefin Polymerization Catalysts Based on Iron and Cobalt. *Chem. Commun.* **1998**, (7), 849–850.

[17] Martínez, J.; Cruz, V.; Ramos, J.; Gutiérrez-Oliva, S.; Martínez-Salazar, J.; Toro-Labbé, A. On the Nature of the Active Site in Bis(imino)pyridyl Iron, a Catalyst for Olefin Polymerization. *J. Phys. Chem. C* **2008**, *112*, 5023–5028.

[18] Raucoules, R.; de Bruin, T.; Raybaud, P.; Adamo, C. Evidence for the Iron(III) Oxidation State in Bis(imino)pyridine Catalysts. A Density Functional Theory Study. *Organometallics* **2008**, *27*, 3368–3377.

[19] Chen, E. Y-X; Marks, T.J. Cocatalysts for Metal-Catalyzed Olefin Polymerization: Activators, Activation Processes, and Structure-Activity Relationships. *Chem. Rev.* **2000**, *100*, 1391–1434.

[20] Zurek, E.; Woo, T.K.; Firman, T.K.; Ziegler, T. Modeling the Dynamic Equilibrium between Oligomers of $(AlOCH_3)_n$ in Methylaluminoxane (MAO). A Theoretical Study Based on a Combined Quantum Mechanical and Statistical Mechanical Approach. *Inorg. Chem.* **2001**, *40*, 361–370.

[21] Zurek, E.; Ziegler, T. A Combined Quantum Mechanical and Statistical Mechanical Study of the Equilibrium of Trimethylaluminum (TMA) and Oligomers of $(AlOCH_3)_n$ Found in Methylaluminoxane (MAO) Solution. *Inorg. Chem.* **2001**, *40*, 3279–3292.

[22] Zurek, E.; Ziegler, T. Toward the Identification of Dormant and Active Species in MAO (Methylaluminoxane)-Activated, Dimethylzirconocene-Catalyzed Olefin Polymerization. *Organometallics* **2002**, *21*, 83–92.

[23] Zohuri, G.H.; Seyedi, S.; Sandaroos, R.; Damavandi, S.; Mohammadi, A. Novel Late Transition Metal Catalysts Based on Iron: Synthesis, Structures and Ethylene Polymerization. *Catal. Lett.* **2010**, *140*, 160–166.

[24] Liu, S. Steric Effect: A Quantitative Description from Density Functional Theory. *J. Chem. Phys.* **2007**, *126*, 244103.

[25] Liu, S.; Govind, N. Toward Understanding the Nature of Internal Rotation Barriers with a New Energy Partition Scheme: Ethane and n-Butane. *J. Phys. Chem. A* **2008**, *112*, 6690–6699.

[26] Tsirelson, V.G.; Stash, A.I.; Liu, S. Quantifying Steric Effect with Experimental Electron Density. *J. Chem. Phys.* **2010**, *133*, 114110.

[27] Esquivel, R.O.; Liu, S.; Angulo, J.C.; Dehesa, J.S.; Antolín, J; Molina-Espíritu, M. Fisher Information and Steric Effect: Study of the Internal Rotation Barrier of Ethane. *J. Phys. Chem. A* **2011**, *115*, 4406–4415.

[28] Huang, Y.; Zhong, A.-G.; Yang, Q.; Liu, S. Origin of Anomeric Effect: A Density Functional Steric Analysis. *J. Chem. Phys.* **2011**, *134*, 084103.

[29] Ess, D.H.; Liu, S.; De Proft, F. Density Functional Steric Analysis of Linear and Branched Alkanes *J. Phys. Chem. A* **2010**, *114*, 12952–12957.

[30] Torrent-Sucarrat, M.; Liu, S.; De Proft, F. Steric Effect: Partitioning in Atomic and Functional Group Contributions. *J. Phys. Chem. A* **2009**, *113*, 3698–3702.

[31] Hohenberg, P.; Kohn, W. Inhomogeneous Electron Gas. *Phys. Rev.* **1964**, *136*, B864–B871.

[32] Kohn, W.; Sham, L.J. Self-Consistent Equations Including Exchange and Correlation Effects. *Phys. Rev.* **1965**, *140*, A1133–A1138.

[33] Chermette, H. Chemical Reactivity Indexes in Density Functional Theory. *J. Comput. Chem.* **1999**, *20*, 129–154.

[34] Geerlings, P.; De Proft, F.; Langenaeker, W. Conceptual Density Functional Theory. *Chem. Rev.* **2003**, *103*, 1793–1874.

[35] Johnson, P.A.; Bartolotti, L.J.; Ayers, P.W.; Fievez, T.; Geerlings, P. Chemical Density and Chemical Reactions: A Unified View from Conceptual DFT. In *Modern Charge-Density Analysis*; Gatti, C., Macchi, P., Eds.; Springer: New York, 2012; Chapter 21, pp 715–764.

[36] Geerlings, P.; Ayers, P.W.; Toro-Labbé, A.; Chattaraj, P.K.; De Proft, F. The Woodward-Hoffmann Rules Reinterpreted by Conceptual Density Functional Theory. *Acc. Chem. Res.* **2012**, *45*, 683–695.

[37] Morell, C.; Grand, A.; Toro-Labbé, A. New Dual Descriptor for Chemical Reactivity. *J. Phys. Chem. A* **2005**, *109*, 205–212.

[38] Ayers, P.W.; Morell, C.; De Proft, F.; Geerlings, P. Understanding the Woodward-Hoffmann Rules by Using Changes in Electron Density. *Chem. Eur. J.* **2007**, *13*, 8240–8247.

[39] Morell, C.; Ayers, P.W.; Grand, A.; Gutiérrez-Oliva, S.; Toro-Labbé, A. Rationalization of Diels-Alder Reactions through the use of the Dual Reactivity Descriptor $\Delta f(\mathbf{r})$. *Phys. Chem. Chem. Phys.* **2008**, *10*, 7239–7246.

[40] Morell, C.; Hocquet, A.; Grand, A.; Jamart-Grégoire, B. A Conceptual DFT Study of Hydrazino Peptides: Assessment of the Nucleophilicity of the Nitrogen

Atoms by means of the Dual Descriptor $\Delta f(\mathbf{r})$. *J. Mol. Struc.–THEOCHEM* **2008**, *849*, 46–51.

[41] Cárdenas, C.; Rabi, N.; Ayers, P.W.; Morell, C.; Jaramillo, P.; Fuentealba, P. Chemical Reactivity Descriptors for Ambiphilic Reagents: Dual Descriptor, Local Hypersoftness, and Electrostatic Potential. *J. Phys. Chem. A* **2009**, *113*, 8660–8667.

[42] Geerlings, P.; De Proft, F. Conceptual DFT: The Chemical Relevance of Higher Response Functions. *Phys. Chem. Chem. Phys.* **2008**, *10*, 3028–3042.

[43] Fuentealba, P.; Parr, R.G. Higher-Order Derivatives in Density-Functional Theory, Especially the Hardness Derivative $\partial\eta/\partial N$. *J. Chem. Phys.* **1991**, *94*, 5559–5564.

[44] De Proft, F.; Ayers, P.W.; Fias, S.; Geerlings, P. Woodward-Hoffmann Rules in Conceptual Density Functional Theory: Initial Hardness Response and Transition State Hardness. *J. Chem. Phys.* **2006**, *125*, 214101–214109.

[45] Parr, R.G.; Yang, W. *Density-Functional Theory of Atoms and Molecules*; Oxford Univ. Press: New York, 1989.

[46] Morell, C.; Grand, A.; Toro-Labbé, A. Theoretical Support for using the $\Delta f(\mathbf{r})$ Descriptor. *Chem. Phys. Lett.* **2006**, *425*, 342–346.

[47] Martínez-Araya, J.I. Why is the Dual Descriptor a More Accurate Local Reactivity Descriptor than Fukui Functions? *J. Math. Chem.* **2015**, *53*, 451–465.

[48] Martínez-Araya; J.I. Revisiting Caffeate's Capabilities as a Complexation Agent to Silver Cation in Mining Processes by means of the Dual Descriptor-A Conceptual DFT Approach. *J. Mol. Model.* **2012**, *18* ,4299–4307.

[49] Liu, S.; Ess, D.H.; Schauer, C.K. Density Functional Reactivity Theory Characterizes Charge Separation Propensity in Proton-Coupled Electron Transfer Reactions. *J. Phys. Chem. A* **2011**, *115*, 4738–4742.

[50] Kumar, N.; Liu, S.; Kozlowski, P.M. Charge Separation Propensity of the Coenzyme B12-Tyrosine Complex in Adenosylcobalamin-Dependent Methylmalonyl-CoA Mutase Enzyme. *J. Phys. Chem. Lett.* **2012**, *3*, 1035–1038.

[51] Flores-Moreno, R. Symmetry Conservation in Fukui Functions. *J. Chem. Theory Comput.* **2010**, *6*, 48–54.

[52] Martínez, J. Local Reactivity Descriptors from Degenerate Frontier Molecular Orbitals. *Chem. Phys. Lett.* **2009**, *478*, 310–322.

[53] Martínez, J.I.; Moncada, J.L.; Larenas, J.M. The Dual Descriptor to measure Local Reactivity on Buckminster Fullerenes: An Analysis within the Framework of Conceptual DFT. *J. Mol. Model.* **2010**, *16*, 1825–1832.

[54] Cárdenas, C.; Ayers, P.W.; Cedillo, A. Reactivity Indicators for Degenerate States in the Density-Functional Theoretic Chemical Reactivity Theory. *J. Chem. Phys.* **2011**, *134*, 174103.

[55] Bultinck, P.; Cardenas, C.; Fuentealba, P.; Johnson, P.A.; Ayers, P.W. How to Compute the Fukui Matrix and Function for Systems with (Quasi-)Degenerate States. *J. Chem. Theory Comp.* **2014**, *10*, 202–210.

[56] Chamorro, E.; Pérez, P.; Duque, M.; De Proft, F.; Geerlings, P. Dual Descriptors within the Framework of Spin-Polarized Density Functional Theory *J. Chem. Phys.* **2008**, *129*, 064117–9.

[57] P. Pérez, E. Chamorro and P.W. Ayers. Universal Mathematical Identities in Density Functional Theory: Results from Three Different Spin-Resolved Representations. *J. Chem. Phys.* **2008**, *128*, 204108–22.

[58] Galván, M.; Vela, A.; Gázquez, J.L. Chemical Reactivity in Spin-Polarized Density Functional Theory. *J. Phys. Chem.* **1988**, *92*, 6470–6474.

[59] Gázquez, J.L.; Galván, M.; Vela, A. Chemical Reactivity in Density Functional Theory: The N-Differentiability Problem. *J. Mol. Struc.–THEOCHEM* **1990**, *210*, 29–38.

[60] Galván, M.; Vargas, R. Spin-Potential in Kohn-Sham Theory. *J. Phys. Chem.* **1992**, *96*, 1625–1630.

[61] Ghanty, T.K.; Ghosh, S.K. Spin-Polarized Generalization of the Concepts of Electronegativity and Hardness and the Description of Chemical Binding. *J. Am. Chem. Soc.* **1994**, *116*, 3943–3948.

[62] Ayers, P. W.; Parr, R. G. Beyond Electronegativity and Local Hardness: Higher-Order Equalization Criteria for Determination of a Ground-State Electron Density *J. Chem. Phys.* **2008**, *129*, 054111.

[63] Labet, V.; Morell, C.; Grand, A.; Cadet, J.; Cimino, P.; Barone, V. Formation of Cross-Linked Adducts between Guanine and Thymine mediated by Hydroxyl Radical and One-Electron Oxidation: A Theoretical Study. *Org. Biomol. Chem.* **2008**, *6*, 3300–3305.

[64] Labet, V.; Morell, C.; Cadet, J.; Eriksson, L.A.; Grand, A. Hydrolytic Deamination of 5-Methylcytosine in Protic Medium. A Theoretical Study. *J. Phys. Chem. A* **2009**, *113*, 2524–2533.

[65] Morell, C.; Grand, A.; Toro-Labbé, A.; Chermette, H. Is Hyper-Hardness more Chemically Relevant than Expected? *J. Mol. Model.* **2013**, *19*, 2893–2900.

[66] Yang, W.; Parr, R.G. Hardness, Softness, and the Fukui Function in the Electronic Theory of Metals and Catalysis. *Proceedings of the National Academy of Sciences* **1985**, *82*, 6723–6726.

[67] Senet, P. Nonlinear Electronic Responses, Fukui Functions and Hardnesses as Functionals of the Ground-State Electronic Density. *J. Chem. Phys.* **1996**, *105*, 6471–6489.

[68] Cardenas, C.; Echegaray, E.; Chakraborty, D.; Anderson, J.S.M.; Ayers, P.W. Relationships between the Third-Order Reactivity Indicators in Chemical Density-Functional Theory. *J. Chem. Phys.* **2009**, *130*, 244105.

[69] Koopmans; T.A. Über die Zuordnung von Wellenfunktionen und Eigenwerten zu den Einzelnen Elektronen Eines Atoms. *Physica* **1933**, *1*, 104–113.

[70] Zielinski, F.; Tognetti, V.; Joubert, L. Condensed Descriptors for Reactivity: A Methodological Study. *Chem. Phys. Lett.* **2012**, *527*, 67–72.

[71] Savin, A.; Umrigar, C.J.; Gonze, X. Relationship of Kohn-Sham Eigenvalues to Excitation Energies. *Chem. Phys. Lett.* **1998**, *288* ,391–395.

[72] Ayers, P.W.; Morrison, R.C.; Parr, R.G. Fermi-Amaldi Model for Exchange-Correlation: Atomic Excitation Energies from Orbital Energy Differences. *Mol. Phys.* **2005**, *103*, 2061–2072.

[73] Martínez-Araya, J.I. Explaining Some Anomalies in Catalytic Activity Values in Some Zirconocene Methyl Cations: Local Hyper-Softness. *J. Phys. Chem. C* **2013**, *117*, 24773–24786.

[74] Hay, P.J.; Wadt, W.R. Ab Initio Effective Core Potentials for Molecular Calculations. Potentials for the Transition Metal Atoms Sc to Hg. *J. Chem. Phys.* **1985**, *82*, 270–283.

[75] Wadt, W.R.; Hay, P.J. Ab Initio Effective Core Potentials for Molecular Calculations. Potentials for Main Group Elements Na to Bi. *J. Chem. Phys.* **1985**, *82*, 284–298.

[76] Hay, P.J.; Wadt, W.R. Ab Initio Effective Core Potentials for Molecular Calculations. Potentials for K to Au Including the Outermost Core Orbitals. *J. Chem. Phys.* **1985**, *82*, 299–310.

[77] Becke, A.D. Density-Functional Thermochemistry. III. The Role of Exact Exchange. *J. Chem. Phys.* **1993**, *98*, 5648–5652.

[78] Lee, C.; Yang, W.; Parr, R.G. Development of the Colle-Salvetti Correlation-Energy Formula into a Functional of the Electron Density. *Phys. Rev. B* **1988**, *37*, 785–789.

[79] Miehlich, B.; Savin, A.; Stoll, H.; Preuss, H. Results obtained with the Correlation Energy Density Functionals of Becke and Lee, Yang and Parr. *Chem. Phys. Lett.* **1989**, *157*, 200–206.

[80] Vosko, S.H.; Wilk, L.; Nusair, M. Accurate Spin-Dependent Electron Liquid Correlation Energies for Local Spin Density Calculations: A Critical Analysis. *Can. J. Phys.* **1980**, *58*, 1200–1211.

[81] Perdew, J.P. Density-Functional Approximation for the Correlation Energy of the Inhomogeneous Electron Gas. *Phys. Rev. B* **1986**, *33*, 8822–8824.

[82] Grimme, S. Semiempirical GGA-type Density Functional Constructed with a Long-Range Dispersion Correction. *J. Comp. Chem.* **2006**, *27*, 1787–1799.

[83] Van Voorhis, T; Scuseria, G.E. A Novel Form for the Exchange-Correlation Energy Functional. *J. Chem. Phys.*, **1998**, *109*, 400-410.

[84] Schlegel; H.B. Optimization of Equilibrium Geometries and Transition Structures. *J. Comput. Chem.* **1982**, *3*, 214–218.

[85] Frisch, M.J.; Trucks, G.W.; Schlegel, H.B.; Scuseria, G.E.; Robb, M.A.; Cheeseman, J.R.; Scalmani, G.; Barone, V.; Mennucci, B.; Petersson, G.A. *et al.*, Gaussian 09, Revision B.01. Gaussian, Inc. Wallingford CT 2009.

[86] Contreras, R.R.; Fuentealba, P.; Galván, M.; Pérez, P. A Direct Evaluation of Regional Fukui Functions in Molecules. *Chem. Phys. Lett.* **1999**, *304*, 405–413.

[87] Fuentealba, P.; Pérez, P.; Contreras, R. On the Condensed Fukui Function. *J. Chem. Phys.* **2000**, *113*, 2544–2551.

[88] Chamorro, E. Fukui, Rev 1.1, 2011.

[89] Chamorro, E.; Pérez, P. Condensed-to-Atoms Electronic Fukui Functions within the Framework of Spin–Polarized Density-Functional Theory. *J. Chem. Phys.* **2005**, *123*, 114107.

[90] Reed, A.E.; Curtiss, L.A.; Weinhold, F. Intermolecular Interactions from a Natural Bond Orbital, Donor-Acceptor Viewpoint. *Chem. Rev.* **1988**, *88*, 899–926.

[91] Breneman, C.M.; Wiberg, K.B. Determining Atom–Centered Monopoles from Molecular Electrostatic Potentials. The Need for High Sampling Density in Formamide Conformational-Analysis *J. Compt. Chem.* **1990**, *11*, 361–373.

[92] Yang, W.; Mortier, W.J. The Use of Global and Local Molecular Parameters for the Analysis of the Gas-Phase Basicity of Amines *J. Am. Chem. Soc.* **1986**, *108*, 5708–5711.

[93] Thanikaivelan, P.; Padmanabhan, J.; Subramanian, V.; Ramasami, T. Chemical Reactivity and Selectivity using Fukui Functions: Basis Set and Population Scheme Dependence in the Framework of B3LYP Theory *Theor. Chem. Acc.* **2002**, *107*, 326–335.

Figure 1: The 2,6–bis(imino)pyridine ligand with different substituent groups represented by $-\mathrm{Y} \in \{-\mathrm{H}, -\mathrm{NO_2}, -\mathrm{OCH_3}\}$.

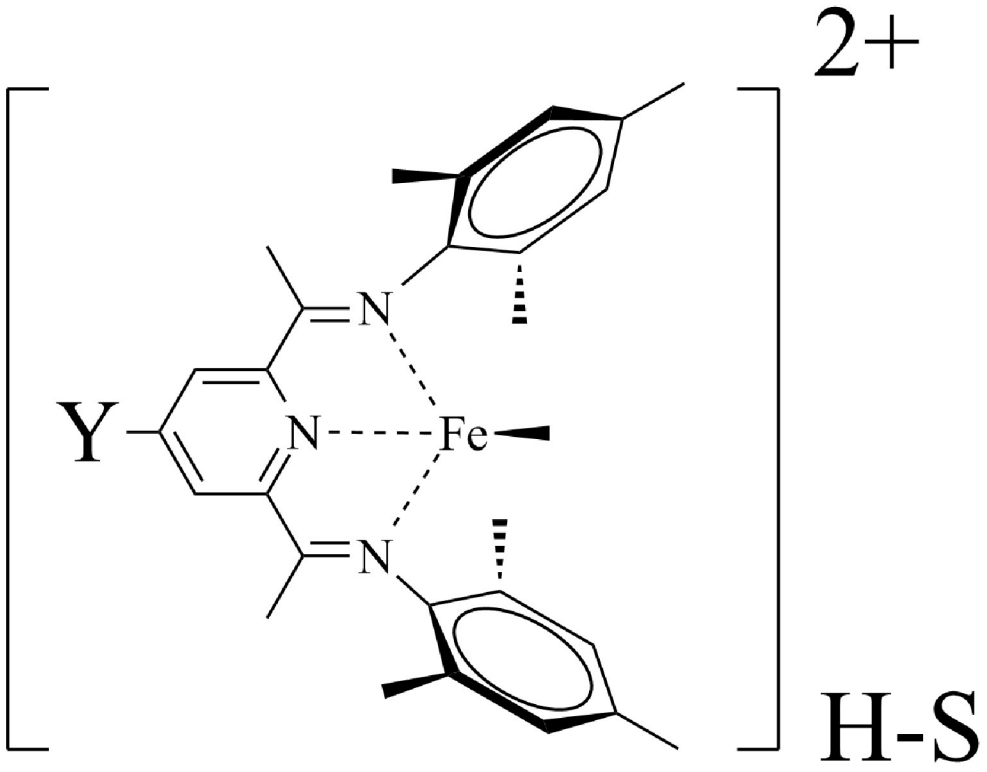

Figure 2: Models of 2,6–bis(imino)pyridil catalysts, also called BIMP-Fe cation, where 2+ is the net electric charge and H-S indicates that it corresponds to a high–spin configuration of sextet type ($2S + 1 = 6$).

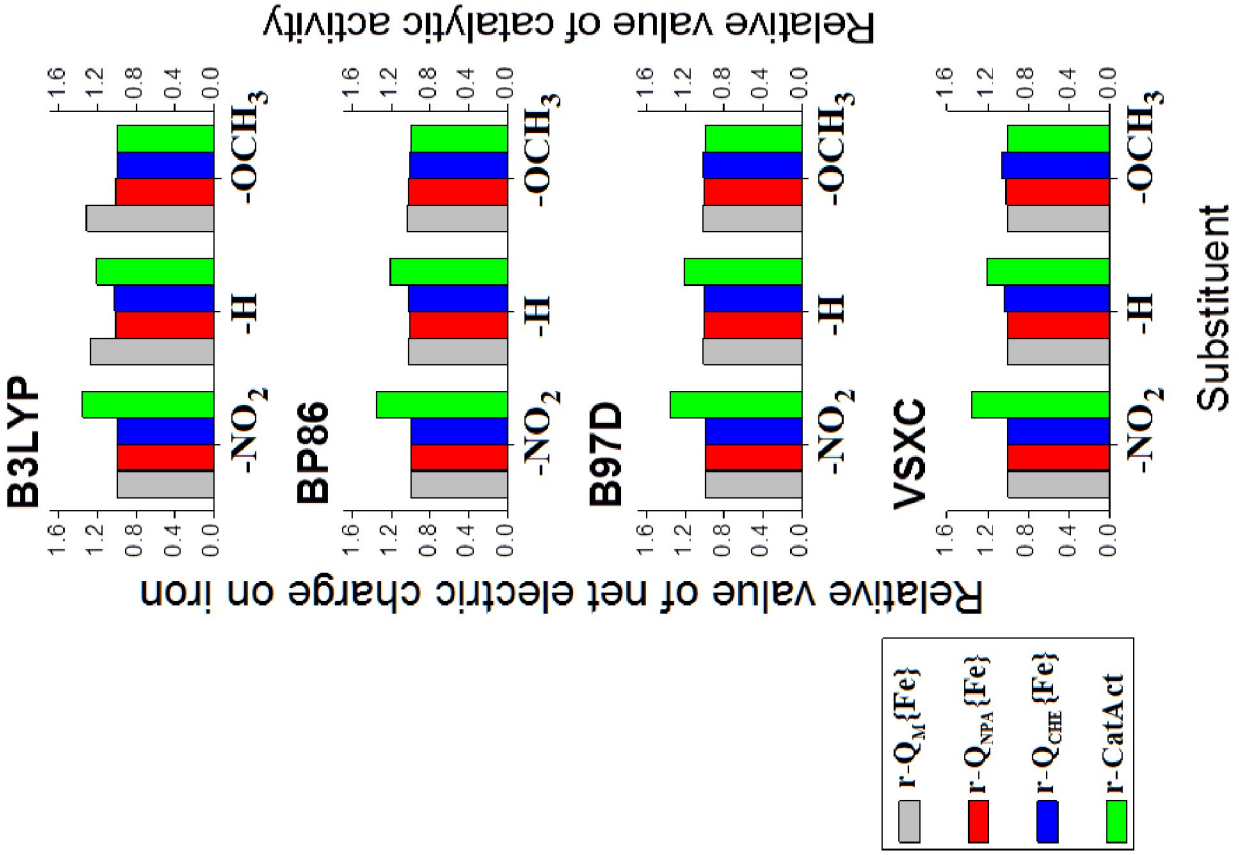

Figure 3: Bar graphs of relative net electric charges on iron atom obtained by means of Mülliken (r-Q_M {Fe}); natural population analysis (r-Q_{NPA} {Fe}) and CHELPG (r-Q_{CHE} {Fe}) along with relative catalytic activity (r-CatAct). These results were obtained by means of different functionals: B3LYP, BP86, B97D and VSXC.

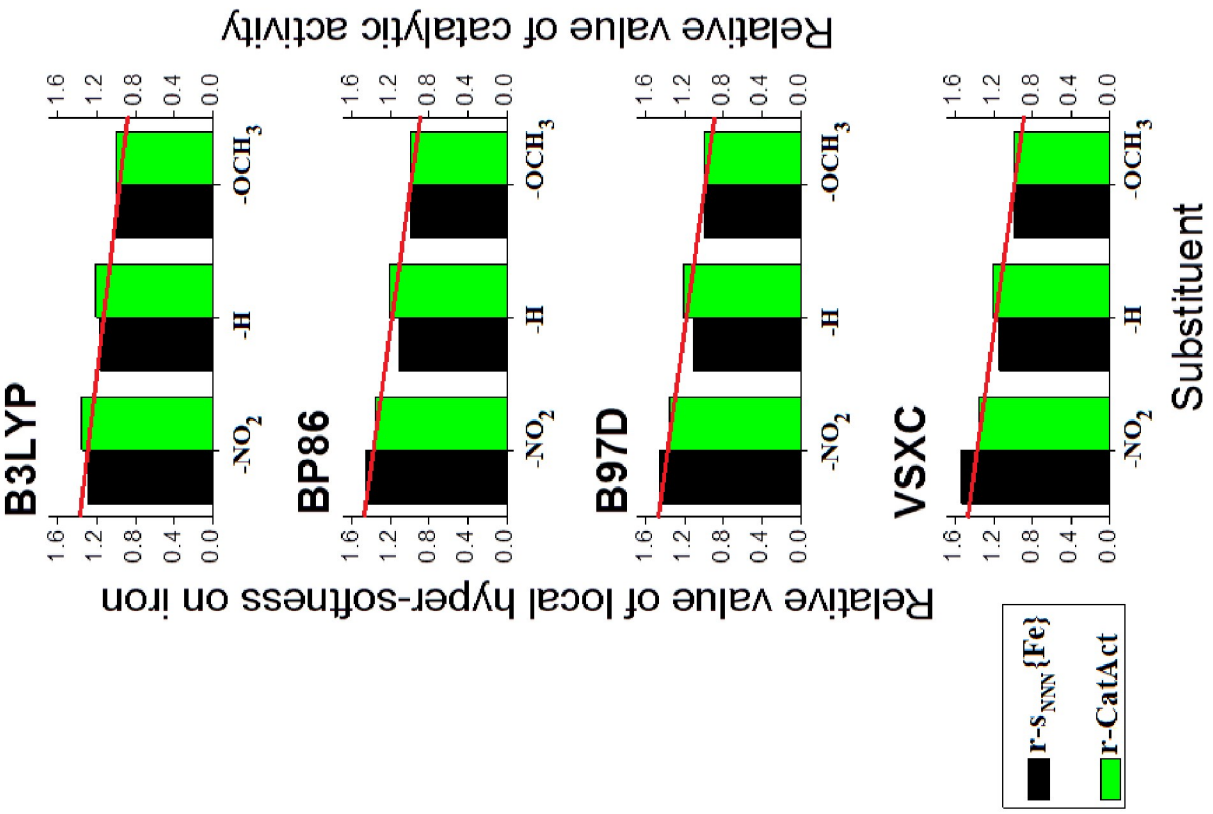

Figure 4: Bar graphs of relative local hyper–softness (r-s_{NNN}{Fe}) condensed on iron atom along with relative catalytic activity (r-CatAct). These results were obtained by means of different functionals: B3LYP, BP86, B97D and VSXC.